

SPARSE ESTIMATION OF THE HEMODYNAMIC RESPONSE FUNCTION IN FUNCTIONAL NEAR INFRARED SPECTROSCOPY

Abd-Krim Seghouane¹ and Adnan Shah²

¹ Department of Electrical and Electronic Engineering, Melbourne School of Engineering, The University of Melbourne. {abd-krim.seghouane@unimelb.edu.au},

² NICTA and The College of Engineering and Computer Science, The Australian National University, Canberra. {adnan.shah@anu.edu.au}.

ABSTRACT

Functional near-infrared spectroscopy (fNIRS) signals offer an interesting alternative to functional magnetic resonance imaging (fMRI) when investigating the temporal dynamics of brain region responses during activations. The hemodynamic response function (HRF) is the object of primary interest to neuroscientists in this case. Making use of a semiparametric model to characterize the oxygenated (HbO) and deoxygenated (HbR) fNIRS time-series and a sparsity assumption on the HRF, a new method for non-parametric HRF estimation from a single fNIRS signal is derived in this paper. The proposed method consistently estimates the HRF using a profile least square estimator obtained using the local polynomial smoothing technique applied to estimate the drift and introducing a regularization penalty in the minimization problem to promote sparsity of the HRF coefficients. The performance of the proposed method is assessed on both simulated and fNIRS data from a finger tapping experiment.

Index Terms— Functional near infrared spectroscopy, hemodynamic response function, sparse estimation, semiparametric model

1. INTRODUCTION

Functional near-infrared spectroscopy (fNIRS) is a non-invasive brain imaging technique that measures functional brain activity through simultaneous recordings of the concentration changes of oxygenated (HbO) and deoxygenated (HbR) hemoglobin. It has shown great potential to analyze cognitive functions in un-restrained environments. Unlike other neuroimaging techniques such as fMRI and EEG, fNIRS provides a balance between temporal and spatial resolution. Furthermore, the independent observation of HbO and HbR in fNIRS measurements and access to their sum as total hemoglobin (HbT) characterizes the governing mechanism of neuronal dynamics in a better way than the blood oxygen level-dependent (BOLD) fMRI signal alone [1]. HbO and HbR are the primary source of signal contrast in fNIRS measurements. These signals are negatively correlated

during neural activations through a mechanism known as neurovascular coupling [2]. Neural activity induces changes in tissue oxygenation which, in turn, modulate the absorption and scattering of the infrared light through the brain tissue. Indeed, HbO and HbR have different attenuation spectra with characteristic properties in the optical window of the near-infrared spectral range 680 – 900 nm [3, 2]. Therefore, different characterizing wavelengths are used in the optical window in fNIRS to differentiate between the two qualitative measures associated with the neural activity. The HbO and HbR as a first approximation are modeled as a convolution of the experimental paradigm characterizing the stimulus by the hemodynamic response function (HRF). HRF models the impulse response of the neurovascular system [4] that is assumed to be linear time-invariant [5].

HRF shape varies considerably across subjects and regions [6] apart from its variability across tasks. Therefore, accurate HRF estimation is essential to characterize the temporal dynamics of brain region response during activations, and the region involvement in functional and effective connectivity [7]. Based on generalized linear model (GLM), the available methods for HRF estimation from fMRI data can be used to estimate the HRF from fNIRS time-series [8]. Among them, nonparametric estimation methods allow more flexibility than parametric HRF estimation methods and offer accuracy in the estimation by inferring the HRF at each time sample [9, 10]. Besides the noise, the estimation of the HRF is further complicated by the presence of drift. Nonparametric methods introduced so far include a parametric part to infer the systematic drift, commonly modeled by polynomials and splines [11] and functions from the discrete cosine transform [10]. However, the relatively un-restrained nature of fNIRS data acquisition system make it susceptible to large head motions than fMRI scanners. This can give rise to severe motion related artifacts that substantially degrade signal quality [12]. Effective HRF estimation requires a modeling approach that efficiently account for the variability of the baseline drift. Though the drift is considered as a nuisance component, its appropriate parametrization is needed for efficient HRF esti-

mation. To yield more accurate estimation of the time course behavior of neuronal responses, a nonparametric approach is also used for the drift estimation in this paper. The use of the nonparametric component for the drift leads to semiparametric inference of the underlying HRF [13].

The HRF estimation methods proposed thus far have considered the dimension of the HRF parameter vector known a priori. However, this parameter is unknown and its estimation should be taken into when estimating the HRF. The HRF can be viewed as a sparse function in time. Using this as prior information, a new consistent HRF estimation method that does not require knowledge of the dimension of the HRF a priori is developed in this paper. The proposed approach uses a profile least square estimator obtained using the local polynomial smoothing technique applied to estimate the drift and a regularization penalty in the minimization problem to promote sparsity of the HRF. The proposed method has the advantage of generating a consistent estimate of the HRF. The performance of the proposed HRF estimation method is assessed on both simulated and experimental fNIRS data from a finger tapping experiment.

2. FNIRS TIME SERIES MODEL

The HbO or HbR signals $\mathbf{y}_i = (y_{i1}, \dots, y_{iN})^\top$ measured in channel C_i over the time course of N acquired samples during an fNIRS experiment characterizes the concentration changes of oxygenated and deoxygenated hemoglobin in that region of the brain. This fNIRS signal is comprised of three components: an experimentally induced controlled activation response, an uncontrolled confound part or a baseline drift (including possible unknown nuisance effects) and a noise term [9, 14, 15]. In matrix form, the fNIRS signal can be described with the following model

$$\mathbf{y}_i = X\theta_i + P\phi_i + \epsilon_i, \quad \epsilon_i \sim N(0, \sigma_\epsilon^2 I_N), \quad (1)$$

where X is a known $(N \times p)$ design matrix consisting of the lagged stimulus covariates. The $(N \times q)$ drift matrix P is a nuisance covariate matrix that takes the potential drift and any other nuisance effect into account. The elements of ϕ_i (for each voxel) are the corresponding coefficients. The parameter vectors θ_i and ϕ_i are unknown p and q dimensional vectors, representing the unknown HRF samples to be estimated and the nuisance variables, respectively. In practice the dimension q can be estimated using a univariate model selection criterion [16, 17, 18]. Assuming pre-whitened measurements, ϵ_i represents independent and identically distributed Gaussian white noise with unknown variance σ_ϵ^2 .

The parametric component $P\phi_i$ is very useful for providing a parsimonious description of the baseline drift. However, it is used at the risk of introducing a modeling bias. Alternatives that offer more flexibility in approximating the drift can be obtained by using a nonparametric component [19]. This

case leads to the use of a semiparametric model for hemodynamic response inference in the presence of unknown smooth drift. In the matrix vector form, this is described by

$$\mathbf{y}_i = X\theta_i + \mathbf{f}_i + \epsilon_i, \quad (2)$$

where $\mathbf{f}_i = (f_i(t_1), \dots, f_i(t_N))^\top$ is a discrete sequence, independent of X , representing the uncontrolled baseline drift including other unknown nuisance effects. Compared with (1) this model has the advantage of not assuming any particular shape for the HRF as well as for the drift function. Taking full advantage of these flexible models will help reduce bias due to model misspecification.

3. HRF ESTIMATION METHOD

In the development that follows, a new approach for HRF estimation in a single channel C_i in the presence of unknown smooth drift is derived for the case of unknown HRF dimension p . While the HRF dimension p is assumed not known, it is set sufficiently large to include the true dimension. Looking closely at a theoretical HRF, of which an example is depicted in Fig. 1, we can observe that it is moderately sparse. Therefore the sparsity assumption is applied to the HRF to develop an efficient HRF estimation algorithm from a single channel data.

The parametric component of model (2) is the primary inter-

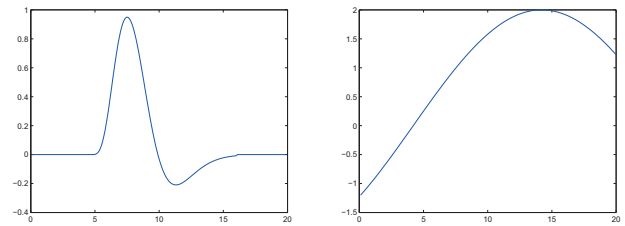


Fig. 1. Illustration of the theoretical HRF (left) and the drift used in the simulation (right)

est. The nonparametric component is a nuisance effect. The proposed HRF estimation procedure make use of the initial estimate

$$\hat{\theta}_i = \left(\sum_{j=1}^{N-1} (X_{j+1} - X_j)^\top (X_{j+1} - X_j) \right)^{-1} \cdot \sum_{j=1}^{N-1} (X_{j+1} - X_j)^\top (y_{i,j+1} - y_{i,j}) \quad (3)$$

obtained using the first order difference time series and the assumption

$$f_i(t_{j+1}) - f_i(t_j) \simeq O\left(\frac{1}{N}\right)$$

obtained by assuming that the drift is a superposition of instrumental and physiological effects that are Lipschitz continuous [20, 21, 15].

Let S be an $N \times N$ a local linear smoothing matrix [22] associated with the time points (t_1, \dots, t_N) whose (i, j) entry is given by

$$S(i, j) = \left(\frac{1}{\sigma}, 0 \right) M^{-1} (1, t_j - t_i)^\top K \left(\frac{(t_j - t_i)}{\sigma} \right)$$

where K is a Gaussian kernel and $\sigma > 0$ is a bandwidth parameter and $M = [Z(t_i)^\top W(t_i) Z(t_i)]$ with

$$W(t) = \frac{1}{\sigma} \text{diag} \left(K \left(\frac{(t_1 - t)}{\sigma} \right), \dots, K \left(\frac{(t_N - t)}{\sigma} \right) \right)$$

and

$$Z(t) = \begin{pmatrix} 1 & t_1 - t \\ \vdots & \vdots \\ 1 & t_N - t \end{pmatrix}.$$

Using an estimate of θ_i ,

$$\mathbf{z}_i = \mathbf{y}_i - X\theta_i \quad (4)$$

can be viewed as an approximation of the noisy drift

$$\mathbf{z}_i \simeq \mathbf{f}_i + \epsilon_i, \quad (5)$$

and an estimate of \mathbf{f}_i using S is given by

$$\hat{\mathbf{f}}_i = S(\mathbf{y}_i - X\theta_i). \quad (6)$$

Substituting (6) in (2) gives

$$(I_N - S)\mathbf{y}_i = (I_N - S)X\theta_i + \epsilon_i \quad (7)$$

where I_N is the identity matrix of size N . Assuming the dimension of θ_i , p known the profile likelihood estimate is similar to the profile least squares estimate and is given by

$$\begin{aligned} \theta_i &= \text{argmin}_{\theta} \|(I_N - S)\mathbf{y}_i - (I_N - S)X\theta\|^2 \\ &= M^{-1} X^\top (I_N - S)^\top (I - S)\mathbf{y}_i \end{aligned} \quad (8)$$

where $M = [X^\top (I_N - S)^\top (I - S)X]$. However, in practice p is unknown. Assuming p is sufficiently large to include the true dimension (8) is used with the sparsity constraint on θ_i

$$\theta_i = \text{argmin}_{\theta_i} \|\mathbf{u}_i - R\theta_i\|^2 + \lambda \sum_{j=1}^p |\theta_{i,j}|. \quad (9)$$

where $R = (I_N - S)X$ and $\mathbf{u}_i = (I_N - S)\mathbf{y}_i$. Each component j of θ_i , is given by

$$\theta_{i,j} = \frac{\text{sign}(|\mathbf{u}_i^\top R_j| - \lambda)_+}{R_j^\top R_j}, \quad j = 1, \dots, p \quad (10)$$

where $(x)_+ = xI(x > 0)$ and R_j is the j^{th} column of R .

Based on the results from [15, 23], the proposed HRF estimator (6) has the advantage of being consistent and easily implementable. It also avoids the selection of nuisance covariates to model the drift.

The proposed HRF estimation algorithm is as follows:

- 1- Generate an initial estimate of θ_i using (3)
- 2- Generate an estimate of the drift using (6)
- 3- Generate the update estimate of θ_i using (10)
- 4- Iterate between 2 and 3 until $\|\theta_i^j - \theta_i^{j+1}\|^2 \leq \delta$

The convergence of the estimator (10) can be analyzed as follows. Relation (3) generates a \sqrt{N} consistent estimator of the HRF θ_i [20][15]. Therefore the estimator of the drift obtained using (6) achieves the optimal rate that can attain \sqrt{N} under certain smoothness conditions of the unknown drift [22]. Based on these results and results from [23] the estimator (10) can achieve \sqrt{N} consistency under certain conditions on λ . Improved convergence results can be obtained by using the adaptive Lasso [24] instead the Lasso in (9).

While (3) produces \sqrt{N} consistent HRF estimation it will tend to have high variance. The proposed approach introduce regularization (bias) to reduce this variance without sacrificing consistency. However, since there is always a cost to pay, this comes at an increase in computational complexity (few iterations of steps 2 and 3 above) and additional conditions on the unknown drift.

4. SIMULATION RESULTS

Simulated event-related fNIRS time series were generated according to

$$y(t_i) = x(t_i) \star h(t) + f(t_i) + \epsilon(t_i) \quad (11)$$

with a single type of stimulus $x(t)$ were used to compare the proposed HRF estimation approach with the method derived in [15] where no sparsity assumption was used. For the simulation, 100 realizations of (11) with $N = 200$, $t_i = \frac{i}{N}$, $i = 1, \dots, 200$ for each variance value of the noise ϵ , σ^2 are used. The stimuli are generated from independent Bernoulli events with $p(x(t_i) = 1) = 0.5$. The true HRF is generated according to [11] with $p = 20$ and is depicted in figure 1. The drift function $f(t_i) = 2\sin(\pi(\frac{i}{N} - 0.21))$, $i = 1, \dots, 200$ is used to simulate the drift and i.i.d samples from a zero mean Gaussian with variance 0.75, 0.5, 0.25, 0.1 and 0.05 were used for $\epsilon_i = \epsilon_{t_i}$. The drift is illustrated in Fig. 1 alongside the HRF.

Table 1 illustrates the estimation results for

$$\frac{1}{p} \|\hat{h} - h_{true}\|^2$$

obtained over the 100 realizations. We can observe that the proposed method outperforms [15]. While it provides an unbiased estimate of the HRF, the method described in [15] exhibits a high variance. It can be observed that the weakness

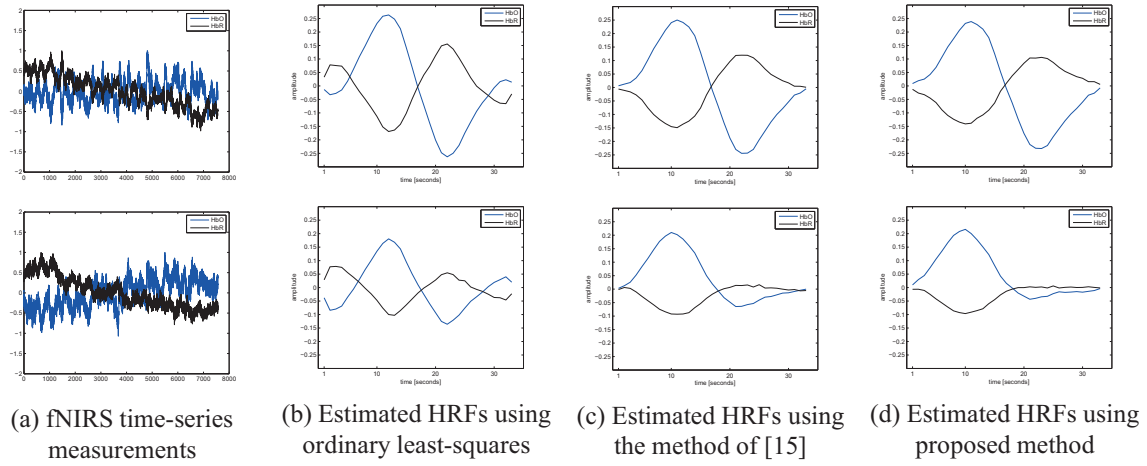


Fig. 3. a) Real fNIRS time-series from activated brain region during finger tapping task: channel 9 (top), channel 15 (bottom). b,c,d) HRF estimates from HbO and HbR responses of these activated channels using b) ordinary least squares, c) the method described in [15], and d) the proposed method. Black color in the sub-figures represents HbR, while Blue represents HbO.

of the method is accentuated as the variance of the noise increases. Results for the proposed method are shown in Fig. 2.

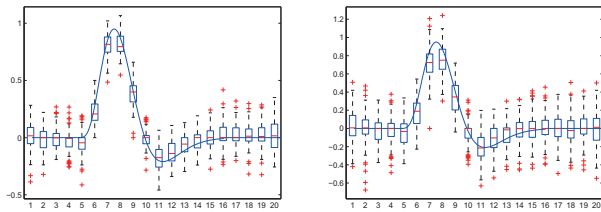


Fig. 2. Boxplots of \hat{h} estimated by the proposed method for $\sigma^2 = 0.1$ (left) and $\sigma^2 = 0.25$ (right), the true HRF is represented by the solid curve.

σ^2	0.05	0.1	0.25	0.5	0.75
Method of [15]	0.170	0.355	0.952	2.053	3.046
Proposed	0.125	0.237	0.593	0.935	1.3661

Table 1. Comparison of the MSE calculated over 100 realizations for the estimated HRF with the proposed method and the method given in [15].

5. RESULTS ON FNIRS DATA

The experiment was performed on ten healthy young adults (mean age 26.9, four males) who performed a finger-tapping task with no head motion (FO), finger tapping with small head motion (FS) and finger tapping with big head motion (FB). All participants gave written informed consent to participate

in this study, which was approved by the Stanford University Institutional Review Board. The aim of the experiment was to investigate the HbO and HbR dynamics during the motor activity finger tapping task. The finger tapping task consisted of 10 alternating tapping and resting epochs. Each tapping epoch lasted 10 s and each resting epoch lasted 20 s (task-period 30 s). Before the start of the experiment, participants were asked to sit relaxed and let their right hand rest naturally on their right knee. When the word “Tap” appeared on the screen, they began tapping all four fingers on their right hand at a rate of 3–4 taps/s till a cue on the screen alerted them to stop. Further details of the experiment can be found in [12]. In this study, we investigated the FS-FB blocks for the concentration change of HbO and HbR for one of the subjects. Apart from the motor activity finger tapping task, further event-related instructions were given to the participants in these blocks. These instructions guided them to move their head in the indicated directions (forward, left, backward and right) supplemented either by “small” for FS-block or “big” for FB-block while kept on performing the tapping task. After delineating the activated region of interest, the resulting activated HbO and HbR signals from the left motor cortex were approached for HRF estimation with the ordinary least squares, the method described in [15], and the proposed method. Results are shown in Figure 3 for two of the channels with different HbO and HbR hemodynamics triggered by underlying neuronal activity in the left motor cortex of the brain. In comparison to ordinary least squares, the method described in [15] and the proposed method are well-adapted to correctly estimate the two different qualitative measures from real fNIRS data. Furthermore, the proposed method offers improvement by further reducing the quadratic error of estimation over [15] as observed from the simulation study.

6. REFERENCES

- [1] G. R. Wylie, H. Graber, G. T. Voelbel, A. D. Kohl, J. DeLuca, Y. Pei, Y. Xu, and R. L. Barbour, "Using co-variations in the Hb signal to detect visual activation: A near infrared spectroscopic imaging study.," *Neuroimage*, vol. 47(2), pp. 473–481, 2009.
- [2] A. Villringer and B. Chance, "Non-invasive optical spectroscopy and imaging of human brain function," *Trends Neurosci.*, vol. 20, pp. 435–442, 1997.
- [3] J. M. Lina, C. Matteau-Pelletier, M. Dehaes, M. Desjardins, and F. Lesage, "Wavelet-based estimation of the hemodynamic responses in diffuse optical imaging.," *Med. Image Anal.*, vol. 4, pp. 606–616, 2010.
- [4] M. M. Plichta, S. Heinzl, C. Ehlis, P. Pauli, and A.J. Fallgatter, "Model-based analysis of rapid event-related functional near-infrared spectroscopy (NIRS) data: A parametric validation study.," *Neuroimage*, vol. 35, pp. 625–634, 2007.
- [5] G. M. Boynton, S. A. Engel, G. H. Glover, and D. J. Heeger, "Linear systems analysis of functional magnetic resonance imaging in human v1.," *The Journal of Neuroscience*, vol. 16, pp. 4207–4221, 1996.
- [6] J. Gonzalez-Castillo, Z. S. Saad, D. A. Handwerker, S. J. Inati, N. Brenowitz, and P. A. Bandettini, "Whole-brain, time-locked activation with simple tasks revealed using massive averaging and model-free analysis," *PNAS*, vol. 109, pp. 5487–5492, 2012.
- [7] A. K. Seghouane and S. I. Amari, "Identification of directed influence: Granger causality, Kullback-Leibler divergence and complexity," *Neural Computation*, vol. 24, pp. 1722–1739, 2012.
- [8] J. Cohen-Adad, S. Chapuisat, J. Doyon, Rossignol, J.-M. Lina, H. Benali, and F. Lesag, "Activation detection in diffuse optical imaging by means of the general linear model," *Medic. Image Anal.*, vol. 11, pp. 616–629, 2007.
- [9] A. K. Seghouane, "A Kullback-Leibler methodology for HRF estimation in fMRI data," *International Conference of the IEEE Engineering in Medicine and Biology Society, EMBC*, pp. 2910–2913, 2010.
- [10] S. Makni, J. Idier, and J. B. Poline, "Joint detection-estimation of brain activity in functional MRI: A multi-channel deconvolution solution," *IEEE Transactions on Signal Processing*, vol. 53, pp. 3488–3502, 2005.
- [11] G. H. Glover, "Deconvolution of impulse response in event-related BOLD fMRI," *Neuroimage*, vol. 9, pp. 416–429, 1999.
- [12] X. Cui, S. Bray, and A. L. Reiss, "Functional near infrared spectroscopy (NIRS) signal improvement based on negative correlation between oxygenated and deoxygenated hemoglobin dynamics," *Neuroimage*, vol. 49, pp. 3039–3046, 2010.
- [13] D. Ruppert, M. P. Wand, and R. J. Carroll, *Semi-parametric regression*, Cambridge University Press, 2003.
- [14] A. K. Seghouane and A. Shah, "HRF estimation in fMRI data with unknown drift matrix by iterative minimization of the Kullback-Leibler divergence," *IEEE Transactions on Medical Imaging*, pp. 192–206, 2012.
- [15] A. Shah and A. K. Seghouane, "Consistent estimation of the hemodynamic response function in fNIRS," *International Conference on Acoustic, Speech and Signal Processing, ICASSP 13*, pp. 1281–1285, 2013.
- [16] A. K. Seghouane and M. Bekara, "A small sample model selection criterion based on the kullback symmetric divergence," *IEEE Transactions on Signal Processing*, vol. 52, pp. 3314–3323, 2004.
- [17] A. K. Seghouane and S. I. Amari, "The AIC criterion and symmetrizing the kullback-leibler divergence," *IEEE Transactions on Neural Networks*, vol. 18, pp. 97–106, 2007.
- [18] A. K. Seghouane, "Asymptotic bootstrap corrections of aic for linear regression models," *Signal Processing*, vol. 90, pp. 217–224, 2010.
- [19] F. G. Meyer, "Wavelet-based estimation of a semi-parametric generalized linear model of fMRI time series," *IEEE Transactions on Medical Imaging*, vol. 22, pp. 315–322, 2003.
- [20] A. Yatchew, "An elementary estimator of the partial linear model," *Economics Letters*, vol. 57, pp. 135–143, 1997.
- [21] A. K. Seghouane and A. Shah, "Estimating the hemodynamic response function estimation in functional MRI by first order differencing," *IEEE International Symposium on Biomedical Imaging, ISBI 13*, pp. 282–285, 2013.
- [22] J. Fan and I. Gijbels, *Local polynomial modelling and its applications*, Chapman and Hall, 1996.
- [23] K. Knight and W. Fu, "Asymptotics for Lasso type estimators," *The Annals of Statistics*, vol. 28, pp. 1356–1378, 2000.
- [24] H. Zou, "The adaptive Lasso and its oracle properties," *Journal of the American Statistical Association*, vol. 101, pp. 1418–1429, 2006.